

Discovery of Small Molecule RIP1 Kinase Inhibitors for the Treatment of Pathologies Associated with Necroptosis

Philip A. Harris,^{*,†} Deepak Bandyopadhyay,[‡] Scott B. Berger,[†] Nino Campobasso,[‡] Carol A. Capriotti,[†] Julie A. Cox,[‡] Lauren Dare,[†] Joshua N. Finger,[†] Sandra J. Hoffman,[†] Kirsten M. Kahler,[§] Ruth Lehr,[‡] John D. Lich,[†] Rakesh Nagilla,[†] Robert T. Nolte,[§] Michael T. Ouellette,[‡] Christina S. Pao,[‡] Michelle C. Schaeffer,[†] Angela Smallwood,[‡] Helen H. Sun,[†] Barbara A. Swift,[†] Rachel D. Totoritis,[‡] Paris Ward,[‡] Robert W. Marquis,[†] John Bertin,[†] and Peter J. Gough[†]

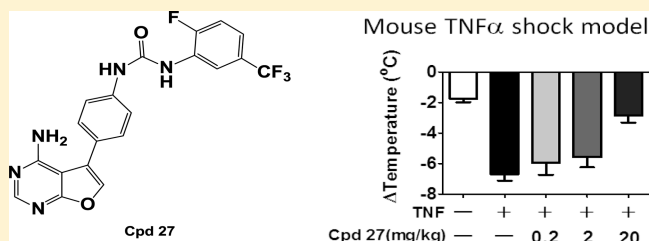
[†]Pattern Recognition Receptor DPU and [‡]Platform Technology & Science, GlaxoSmithKline, Collegeville Road, Collegeville, Pennsylvania 19426, United States

[§]Platform Technology & Science, GlaxoSmithKline, Research Triangle Park, North Carolina 27709, United States

Supporting Information

ABSTRACT: Potent inhibitors of RIP1 kinase from three distinct series, 1-aminoisoquinolines, pyrrolo[2,3-b]pyridines, and furo[2,3-d]pyrimidines, all of the type II class recognizing a DLG-out inactive conformation, were identified from screening of our in-house kinase focused sets. An exemplar from the furo[2,3-d]pyrimidine series showed a dose proportional response in protection from hypothermia in a mouse model of TNF α induced lethal shock.

KEYWORDS: RIP1, type II kinase inhibitors, necroptosis



Necrosis is a highly inflammatory form of cell death that is thought to be involved in the pathogenesis of a wide variety of human diseases.¹ The inflammation induced by necrotic cell death is primarily due to disruption of the plasma membrane and the unregulated leakage of danger associated molecular patterns (DAMPs), intracellular components that potentially activate the innate immune system when released into the extracellular matrix.² Historically, necrosis has been considered an uncontrolled form of cell death that is refractory to therapeutic intervention. However, more recent work has shown that necrosis can be a programmed and tightly regulated event, which offers a novel opportunity for the treatment of diseases driven by necrotic cell death.

One form of orchestrated necrotic cell death, termed programmed necrosis (or necroptosis), is induced by TNF α and dependent upon RIP1 (receptor interacting protein 1) kinase activity.³ This pathway was initially identified following a cell based screen in which Degterev et al. identified a series of small molecules, termed Necrostatins, that blocked the necrotic death of human monocytic U937 cells induced by treatment with TNF α and the caspase inhibitor zVAD.fmk.⁴ These were subsequently identified as RIP1 kinase inhibitors⁵ and were shown to have efficacy in animal models of ischemia/reperfusion injury in the brain,⁶ retina,⁷ and kidney,⁸ as well as models of myocardial infarction⁹ and retinal detachment.¹⁰ Recent data from genetically manipulated mouse models has further highlighted the role for RIP1-dependent necroptosis as a key driver of the pathogenesis of inflammation and disease in the intestine and the skin.^{11–13} Additionally, the effects of RIP1

kinase activity are not limited to cell death, as RIP1 kinase activity has also been implicated as a direct driver of proinflammatory cytokine production.¹⁴

Recently, Shi et al. have reported the cocrystal structures of several necrostatins bound in a hydrophobic pocket between the N- and C-lobes of the Rip1 kinase domain. These inhibitors interact with highly conserved amino acids in the activation loop and surrounding structural elements to stabilize RIP1 in an inactive conformation.¹⁵

The reported Necrostatins have moderate potency and poor pharmacokinetic properties rendering them unsuitable for development as therapeutics. In order to identify novel inhibitors of RIP1 kinase activity, we developed a fluorescence polarization (FP) biochemical assay. Since expression of the full length protein containing the death domain led to insoluble protein, not suitable for assay development, we used the kinase domain of RIP1 (1–375).

Screening of the GSK kinase inhibitor libraries identified a number of inhibitors of RIP1 characteristic of the type II kinase inhibitor class that target the inactive DFG-out conformation.¹⁶ This conserved DFG (Asp-Phe-Gly) sequence (or more rarely D[LWY]G) is located immediately before the activation loop and it adopts a different conformation in which the aspartate and phenylalanine side chains change positions and point in

Received: September 25, 2013

Accepted: November 4, 2013

Published: November 4, 2013

opposite directions compared to the active “DFG-in” orientation. The phenylalanine moves inward to partially obstruct the ATP-binding site. This rearrangement creates a new hydrophobic allosteric binding pocket, adjacent to the ATP-binding site. In RIP1 this Asp-Phe-Gly sequence on the activation loop is Asp-Leu-Gly (DLG).

Some common features are present in these type II kinase inhibitors as shown in Figure 1. They contain a heterocycle that

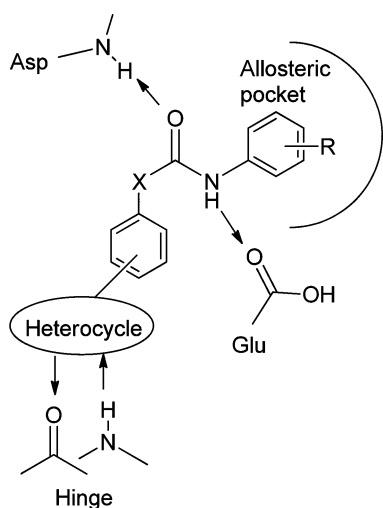


Figure 1. Binding modes of type II kinase inhibitors.

forms one or two hydrogen bonds with the kinase hinge residue and a hydrophobic aryl moiety occupying the new allosteric hydrophobic pocket. In addition, the inhibitors contain an aryl urea (or amide) moiety linking the hinge-binding heterocycle to the hydrophobic moiety, which makes additional hydrogen bond interactions to an aspartate-backbone NH and a highly conserved glutamate side chain of the α -C helix.¹⁷

Several series that are characteristic of type II kinase inhibitors were identified from the GSK kinase screening sets; whereas only a single type I series was identified with a very poor kinase selectivity profile. The superior kinase selectivity profile of the type II inhibitors is thought to be due to the amino acid residues around the newly formed hydrophobic binding pocket being less conserved compared to the residues that form the ATP binding pocket.¹⁸ The type II series profiled in Table 1 have a 1-aminoisoquinoline as the hinge binder and a meta-(trifluoromethyl)phenyl as the hydrophobic aryl moiety.¹⁹ The meta (trifluoromethyl)-phenyl is a common moiety found in multiple type II kinase inhibitors, such as the VEGFR2/b-Raf inhibitors Sorafenib and Regorafenib, and is thought to target a conserved hydrophobic subpocket in the allosteric site.¹⁷ In addition to the trifluoromethyl meta substituent, fluoro-substitution around the aryl ring led to modest changes in potency except at the 2-position (compound 5) where activity was largely lost. Substitution at the 6-position by chlorine also led to a large drop off in potency (compound 7). However, replacement of the meta-(trifluoromethyl)-phenyl with a *tert*-butylisoxazole (compound 8) showed equivalent efficacy.

In addition to the FP binding assay we also utilized an ADP-Glo kinase activity assay, a luminescent kinase assay measuring the ADP formed during autophosphorylation of RIP1. In general the potency of the compounds in both the FP binding assay and the ADP-Glo activity assay correlated reasonably well.

Table 1. 1-Aminoisoquinolines

Cpd	Ar	RIP1 FP	ADP-Glo IC ₅₀ (μM)	U937
1		0.02	0.025	0.63
2		0.013	0.13	0.63
3		0.16	0.025	2.5
4		0.32	0.01	2.5
5		>10	4.0	>10
6		0.04	0.16	2.0
7		3.2	0.63	>10
8		0.016	0.01	0.63

To measure cellular activity we examined the ability of our active compounds to prevent the necrotic death of human monocytic U937 cells induced by treatment with TNF α and the caspase inhibitor zVAD.fmk, as described by Degterev et al.⁴ In general the potency of the compounds in the cell based assay were about 10–50-fold weaker than the biochemical potencies. In this series, the optimal inhibitors in terms of both biochemical and cellular potencies were compounds 1 and 8. However, the moderate cellular potencies observed did not support advancing this series into in vivo models.

To confirm the binding mode of this series in RIP1, we obtained a cocrystal structure of compound 8 bound in RIP1 (1–324) as shown in Figure 2. Structure determination was done by molecular replacement using the atomic coordinates of

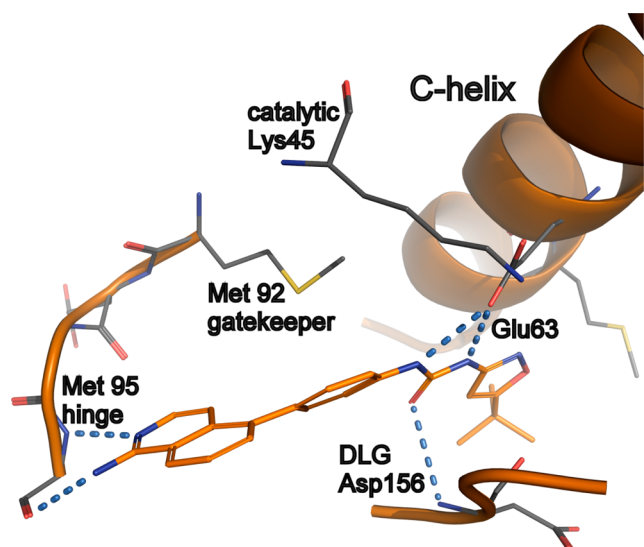


Figure 2. Co-crystal structure of Rip1 (1–324) and 1-aminoisoquinoline 8.

LIMK1 kinase domain (PDB code 4NEU) as a search model (see Supporting Information for details). The X-ray structure of the RIP1 kinase domain was refined to 2.6 Å resolution (Figures 2 and S1–3 and Table S1, Supporting Information). There are two molecules in the asymmetric unit referred to as molecule A and B, respectively. Both chains are similar enough for discussion of one chain. RIP1 (1–324) model has the canonical kinase fold with an N-lobe and a C-lobe connected by an intervening hinge. Residues 166–187 of the activation loop and the N- and C-termini are disordered and not modeled. The model starts at residue 7 and ends at residue 313.

The X-ray structure confirms compound 8 is a type II kinase inhibitor and binds to a DLG-out inactive form of RIP1, distinct than the inactive conformation observed for Rip1 cocrystallized with the necrostatins.¹⁵ The 1-aminoisoquinoline heterocycle of 8 is a two point hinge binder and forms H-bonds to the backbone N and CO of residue Met 95. The isoquinoline is sandwiched between Tyr 94 and Ile43 on one side and Leu145 on the opposite face. A bifurcated H-bond occurs between the side chain of Glu63 and the urea portion of 8. Glu63 is part of the c-helix, common to kinases. A fourth H-bond occurs between the backbone amide of Asp156 and the carbonyl oxygen of the urea. Asp156 is part of the DLG motif. The isoxazole heterocycle sits deep in the allosteric pocket created by the DLG-out conformation and partially defined by the C-helix. The pocket is extremely hydrophobic and defined by amino acids Met66, Met67 (C-helix), Leu70, Val75 (loop following C-helix), Leu129, Val134 (catalytic loop), and Leu159 (after DLG). The *tert*-butyl group resides in a mostly hydrophobic subpocket comprising Leu70, Val75, Val76, Leu129, Val134, His136, Ile154, and Ala155.

A second series identified from screening utilized the 5-phenylpyrrolo[2,3-*b*]pyridine heterocycle as the hinge binder, as shown in Table 2.²⁰ The unsubstituted urea (compound 9) had only weak potency, but small substitutions at the 3-position (entries 10–14) gave up to 1000-fold increase in activity. These small groups are presumably targeting the same lipophilic subpocket where the *tert*-butyl group of the 1-aminoisoquinolines series was shown to occupy in the cocrystal structure shown in Figure 2. With regards to both enzymatic and cellular potencies, the 3-trifluoromethyl substitution was

Table 2. 5-Phenylpyrrolo[2,3-*b*]pyridines

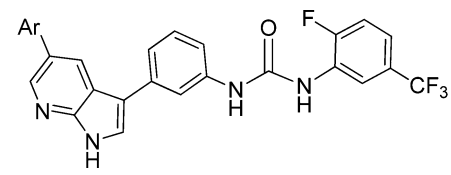
Cpd	Ar	RIP1 FP	ADP-Glo	U937
		IC ₅₀ (μM)		
9		1.3	0.40	0.60
10		0.020	0.013	0.16
11		0.016	0.016	0.32
12		0.032	0.032	0.079
13		0.032	0.0063	0.40
14		0.013	0.01	0.32
15		0.20	0.080	0.16
16		2.0	0.50	7.9

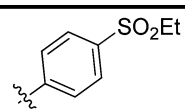
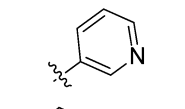
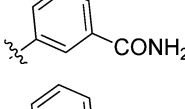
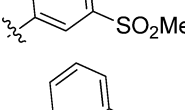
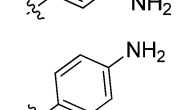
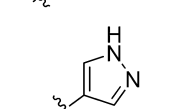
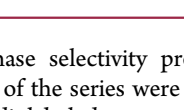
optimal. The nonaromatic cyclopentyl urea (compound 16) had weak activity.

Table 3 shows the SAR resulting from substitution at the aryl ring at the 5-position of the pyrrolo[2,3-*b*]pyridine, with a 5-fluoro-3-(trifluoromethyl)phenyl ring at the urea occupying the hydrophobic pocket. In general, activity was well maintained with the meta-pyridyl (compound 18) giving excellent potencies in both the biochemical ADP-Glo (4 nM) and cellular U937 (6.3 nM) assays. Despite their excellent *in vitro* potencies, both the pyrrolo[2,3-*b*]pyridines 18 and 20 had minimal systemic oral exposures when examined in both rat and mouse which would not support evaluation in an *in vivo* model.

A third series we identified with a more promising pharmacokinetic profile was the furo[2,3-*d*]pyrimidines as detailed in Table 4.²¹ The SAR around the urea shows similar preference for small groups at the meta position as observed in the previous series. As observed with the 1-aminoisoquinolines series, fluoro substitution at the 2 position (compound 28) or chloro substitution at 6 position (compound 30) were detrimental to potency. Similar to compound 8 in the 1-aminoisoquinoline series, incorporation of the *tert*-butylisoxazole urea 35 was favorable and quite comparable to the 5-fluoro-3-(trifluoromethyl)phenyl urea 27.

Table 3. 5-Arylpyrrolo[2,3-b]pyridines

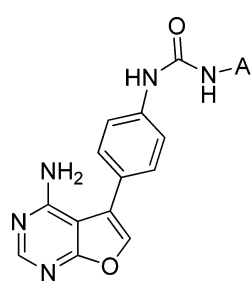


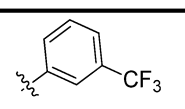
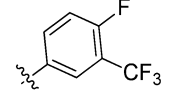
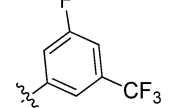
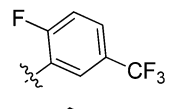
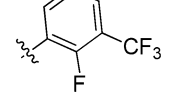
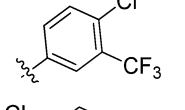
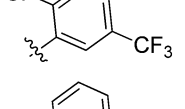
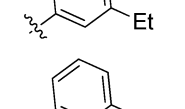
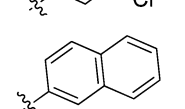
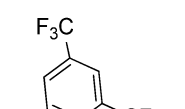
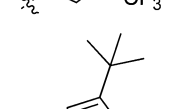
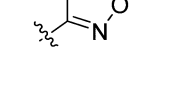
Cpd	Ar	RIP1 FP	ADP-Glo	U937
		IC ₅₀ (μM)		
17		0.0032	0.010	0.025
18		0.0079	0.0040	0.0063
19		0.016	0.010	0.063
20		0.063	0.010	0.050
21		0.0013	0.032	0.016
22		0.032	0.050	0.016
23		0.016	0.006	0.063

The kinase selectivity profiles of representative exemplars from each of the series were obtained against 300 kinases using a P33 radiolabeled assay at Reaction Biology Corporation (RBC).²² Each compound was tested at 1 μM concentration in duplicate against each kinase with 10 μM ATP and >50% inhibition was defined as being active. RIP1 kinase was not included in this RBC selectivity panel. The pyrrolo[2,3-b]pyridine series showed the highest kinase selectivity, with two exemplars **17** and **18** inhibiting 7 and 15 of the 300 kinases, respectively. The furo[2,3-d]pyrimidine **27** inhibited 25 kinases of the 300 assayed at 1 μM. The least selective series was the 1-aminoisoquinolines, with compounds **1** and **8** showing activity against 30 and 46 kinases, respectively.

The furo[2,3-d]pyrimidine **27** possessed good systemic exposure in the mouse following oral administration with an AUC of 14 ± 7 μg·h/mL and a C_{max} of 1100 ng/mL at 4 h (Figure 3). Compound **27** was therefore selected for further evaluation in vivo using a mouse model of TNFα induced lethal shock. In this model, injection of TNFα leads to a systemic inflammatory response, characterized by hypotension, hepatitis, hypothermia, and bowel necrosis. Duprez et al. have reported that the RIP1 kinase inhibitor necrostatin, administered intravenously, showed significant protection from hypothermia and death in this model.²³ Compound **27** was dosed orally 15 min prior to TNFα injection and showed 15%, 22%, and 77% protection from body temperature loss over 7 h, compared to TNFα alone, at doses of 0.2, 2.0, and 20 mg/kg, respectively

Table 4. Furo[2,3-d]pyrimidines



Cpd	Ar	RIP1 FP	ADP-Glo	U937
		IC ₅₀ (μM)		
24		0.02	0.010	1.0
25		0.16	0.50	1.3
26		0.13	0.063	5.0
27		0.063	0.013	0.25
28		0.25	0.20	10
29		0.16	0.032	1.3
30		>10	2.5	>10
31		0.025	0.010	0.25
32		0.16	0.20	7.9
33		0.10		0.79
34		0.32	0.032	7.9
35		0.032	0.016	0.20

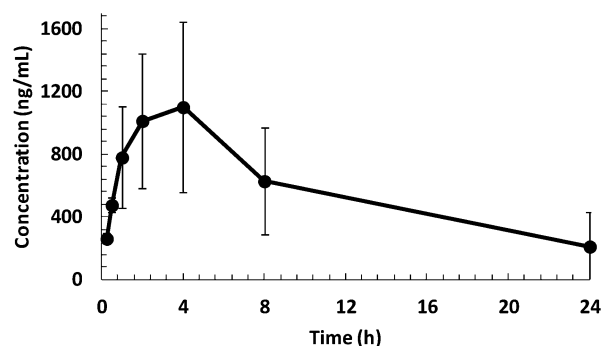


Figure 3. Average (\pm standard deviation) blood concentrations of compound 27 following oral administration (2.0 mg/kg) in the male C57BL/6 mouse.

(Figure 4). Compound 27 has a relatively moderate molecular weight (431.3) and ClogP (4.2) and good permeability (210

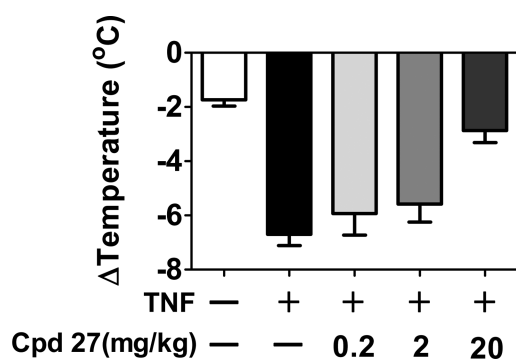


Figure 4. Evaluation of compound 27 in mouse TNF α induced lethal shock model measuring reduction in body temperature loss.

nm/sec), but requires further lead optimization to address its low solubility (13 μ M) and high protein binding (0.04% free fraction in mouse).

In conclusion, we have identified 3 distinct type II inhibitors of RIP1 kinase (1-aminoisoquinolines, pyrrolo[2,3-b]pyridines, and furo[2,3-d]pyrimidines) with potent activity in both biochemical and cellular assays. A cocrystal structure of a 1-aminoisoquinoline in the RIP1 kinase domain shows the inhibitor occupying the ATP binding pocket with the kinase adopting a DLG-out conformation. An exemplar from the furo[2,3-d]pyrimidine series showed excellent mouse exposure dosed orally and gave a dose proportional response in protection from hypothermia in a mouse model of TNF α induced lethal shock. Further exploration of these promising RIP1 kinase inhibitors is underway to determine their utility in the clinic.

■ ASSOCIATED CONTENT

Supporting Information

Details of the synthesis and spectroscopic characterization of all compounds and intermediates, kinase selectivity data together with protocols for biological experiments, and crystallographic information. This material is available free of charge via the Internet at <http://pubs.acs.org>.

Accession Codes

The atomic coordinates and structure factors of RIP1 bound to compound 8 have been deposited in the Protein Data Bank with accession code 4NEU.

■ AUTHOR INFORMATION

Corresponding Author

*(P.A.H.) E-mail: philip.a.harris@gsk.com.

Author Contributions

All authors have given approval to the final version of the manuscript.

Notes

All studies involving the use of animals were conducted after review by the GlaxoSmithKline (GSK) Institutional Animal Care and Use Committee and in accordance with the GSK Policy on the Care, Welfare, and Treatment of Laboratory Animals.

The authors declare the following competing financial interests: All authors are current employees and stockholders of GlaxoSmithKline.

■ ABBREVIATIONS

RIP, receptor interacting protein; TNF α , tumor necrosis factor alpha; DFG, aspartic acid-phenylalanine-glycine; DLG, aspartic acid-leucine-glycine; zVAD.fmk, *N*-benzyloxycarbonyl-Val-Ala-Asp(O-Me) fluoromethyl ketone; FP, fluorescence polarization; VEGFR, vascular endothelial growth factor receptor; b-RAF, rapidly accelerated fibrosarcoma; ADP, adenosine diphosphate; ATP, adenosine triphosphate; AUC, area under the curve

■ REFERENCES

- Iyer, S. S.; Pulskens, W. P.; Sadler, J. J.; Butter, L. M.; Teske, G. J.; Ulland, T. K.; Eisenbarth, S. C.; Florquin, S.; Flavell, R. A.; Leemans, J. C.; Sutterwala, F. S. Necrotic cells trigger a sterile inflammatory response through the Nlrp3 inflammasome. *Proc. Natl. Acad. Sci. U.S.A.* **2009**, *106*, 20388–20393.
- Bianchi, M. E. DAMPs, PAMPs and alarmins: all we need to know about danger. *J. Leukocyte Biol.* **2007**, *81*, 1–5.
- Galluzzi, L.; Kroemer, G. Necroptosis turns TNF lethal. *Immunity* **2011**, *35*, 849–851.
- Degterev, A.; Huang, Z.; Boyce, M.; Li, Y.; Jagtap, P.; Mizushima, N.; Cuny, G. D.; Mitchison, T. J.; Moskowitz, M. A.; Yuan, J. Chemical inhibitor of nonapoptotic cell death with therapeutic potential for ischemic brain injury. *Nat. Chem. Biol.* **2005**, *1*, 112–119.
- Degterev, A.; Hitomi, J.; Germscheid, M.; Ch'en, I. L.; Korkina, O.; Teng, X.; Abbott, D.; Cuny, G. D.; Yuan, C.; Wagner, G.; Hedrick, S. M.; Gerber, S. A.; Lugovskoy, A.; Yuan, J. Identification of RIP1 kinase as a specific cellular target of necrostatins. *Nat. Chem. Biol.* **2008**, *4*, 313–321.
- Xu, X.; Chua, K. W.; Chua, C. C.; Liu, C. F.; Hamdy, R. C.; Chua, B. H. Synergistic protective effects of humanin and necrostatin-1 on hypoxia and ischemia/reperfusion injury. *Brain Res.* **2010**, *1355*, 189–194.
- Rosenbaum, D. M.; Degterev, A.; David, J.; Rosenbaum, P. S.; Roth, S.; Grotta, J. C.; Cuny, G. D.; Yuan, J.; Savitz, S. I. Necroptosis, a novel form of caspase-independent cell death, contributes to neuronal damage in a retinal ischemia-reperfusion injury model. *J. Neurosci. Res.* **2010**, *88*, 1569–1576.
- Linkermann, A.; Bräsen, J. H.; Himmerkus, N.; Liu, S.; Huber, T. B.; Kunzendorf, U.; Krautwald, S. Rip1 (receptor-interacting protein kinase 1) mediates necroptosis and contributes to renal ischemia/reperfusion injury. *Kidney Int.* **2012**, *81*, 751–761.
- Smith, C. C.; Davidson, S. M.; Lim, S. Y.; Simpkin, J. C.; Hothersall, J. S.; Yellon, D. M. Necrostatin: a potentially novel cardioprotective agent? *Cardiovasc. Drugs Ther.* **2007**, *21*, 227–233.
- Trichonas, G.; Murakami, Y.; Thanos, A.; Morizane, Y.; Kayama, M.; Debouck, C. M.; Hisatomi, T.; Miller, J. W.; Vavvas, D. G. Receptor interacting protein kinases mediate retinal detachment-

induced photoreceptor necrosis and compensate for inhibition of apoptosis. *Proc. Natl. Acad. Sci. U.S.A.* **2010**, *107*, 21695–21700.

(11) Günther, C.; Martini, E.; Wittkopf, N.; Amann, K.; Weigmann, B.; Neumann, H.; Waldner, M. J.; Hedrick, S. M.; Tenzer, S.; Neurath, M. F.; Becker, C. Caspase-8 regulates TNF- α -induced epithelial necroptosis and terminal ileitis. *Nature* **2011**, *477*, 335–339.

(12) Welz, P. S.; Wullaert, A.; Vlantis, K.; Kondylis, V.; Fernández-Majada, V.; Ermolaeva, M.; Kirsch, P.; Sterner-Kock, A.; van Loo, G.; Pasparakis, M. FADD prevents RIP3-mediated epithelial cell necrosis and chronic intestinal inflammation. *Nature* **2011**, *477*, 330–334.

(13) Bonnet, M. C.; Preukschat, D.; Welz, P. S.; van Loo, G.; Ermolaeva, M. A.; Bloch, W.; Haase, I.; Pasparakis, M. The adaptor protein FADD protects epidermal keratinocytes from necroptosis in vivo and prevents skin inflammation. *Immunity* **2011**, *35*, 572–582.

(14) Lukens, J. R.; Vogel, P.; Johnson, G. R.; Kelliher, M. A.; Iwakura, Y.; Lamkanfi, M.; Kanneganti, T. D. RIP1-driven autoinflammation targets IL-1 α independently of inflammasomes and RIP3. *Nature* **2013**, *498*, 224–227.

(15) Xie, T.; Peng, W.; Liu, Y.; Yan, C.; Maki, J.; Degterev, A.; Yuan, J.; Shi, Y. Structural basis of RIP1 inhibition by necrostatins. *Structure* **2013**, *21*, 493–499.

(16) Kufareva, I.; Abagyan, R. Type-II kinase inhibitor docking, screening, and profiling using modified structures of active kinase states. *J. Med. Chem.* **2008**, *51*, 7921–7932.

(17) Liu, Y.; Gray, N. S. Rational design of inhibitors that bind to inactive kinase conformations. *Nat. Chem. Biol.* **2006**, *2*, 358–364.

(18) Davis, M. I.; Hunt, J. P.; Herrgard, S.; Ciceri, P.; Wodicka, L. M.; Pallares, G.; Hocker, M.; Treiber, D. K.; Zarrinkar, P. P. Comprehensive analysis of kinase inhibitor selectivity. *Nat. Biotechnol.* **2011**, *29*, 1046–1051.

(19) Washio, Y. Preparation of Aryl Substituted Isoquinoline Derivatives As Inhibitors of VEGFR2, TIE-2, and EphB4. *PCT Int. Appl.* WO2005049576, 2005.

(20) Patnaik, S.; Stevens, K. L.; Gerding, R.; Deanda, F.; Shotwell, J. B.; Tang, J.; Hamajima, T.; Nakamura, H.; Leesnitzer, M. A.; Hassell, A. M.; Shewchuck, L. M.; Kumar, R.; Lei, H.; Chamberlain, S. D. Discovery of 3,5-disubstituted-1H-pyrrolo[2,3-b]pyridines as potent inhibitors of the insulin-like growth factor-1 receptor (IGF-1R) tyrosine kinase. *Bioorg. Med. Chem. Lett.* **2009**, *19*, 3136–3140.

(21) Miyazaki, Y.; Tang, J.; Maeda, Y.; Nakano, M.; Wang, L.; Nolte, R. T.; Sato, H.; Sugai, M.; Okamoto, Y.; Truesdale, A. T.; Hassler, D. F.; Nartey, E. N.; Patrick, D. R.; Ho, M. L.; Ozawa, K. Orally active 4-amino-5-diarylurea-furo[2,3-d]pyrimidine derivatives as anti-angiogenic agent inhibiting VEGFR2 and Tie-2. *Bioorg. Med. Chem. Lett.* **2007**, *17*, 1773–1778.

(22) Reaction Biology Corp. <http://www.reactionbiology.com>.

(23) Duprez, L.; Takahashi, N.; Van Hauwermeiren, F.; Vandendriessche, B.; Goossens, V.; Vanden Berghe, T.; Declercq, W.; Libert, C.; Cauwels, A.; Vandenabeele, P. RIP kinase-dependent necrosis drives lethal systemic inflammatory response syndrome. *Immunity* **2011**, *35*, 908–918.